Radiomics analysis of [^{18}F]-fluoro-2-deoxyglucose positron emission tomography for the prediction of cervical lymph node metastasis in tongue squamous cell carcinoma

Takaharu Kudoh[1*], Akihiro Haga[2], Keiko Kudoh[1], Akira Takahashi[1], Motoharu Sasaki[3], Yasusei Kudo[4], Hitoshi Ikushima[3], and Youji Miyamoto[1]

[1] Department of Oral Surgery, Tokushima University Graduate School of Biomedical Sciences, Kuramoto-cho, Tokushima, Japan

[2] Department of Medical Image Information Science, Tokushima University Graduate School of Biomedical Sciences, Kuramoto-cho, Tokushima, Japan

[3] Department of Therapeutic Radiology, Tokushima University Graduate School of Biomedical Sciences, Kuramoto-cho, Tokushima, Japan

[4] Department of Oral Bioscience, Tokushima University Graduate School of Biomedical Sciences, Kuramoto-cho, Tokushima, Japan

***Corresponding Author:** Takaharu Kudoh (kudoh@tokushima-u.ac.jp)

Declarations

Funding

This work was supported by Grants-in-Aid for Scientific-Research (grant number 19K10268).

Conflicts of interest/Competing interests

The authors declare no conflicts of interest.

Ethics approval

The study was approved by the ethics committee of the Tokushima University (approval number 3212, date of approval July 23, 2018), and the study protocol was performed in accordance to the Declaration of Helsinki.

Informed consent

The requirement for informed consent was waived by the institutional review board owing to the retrospective nature of the study.

Data availability

The data that support the findings of this study are available from the corresponding author, TK, upon reasonable request.

Author contributions

All authors contributed to the study conception and design. Material preparation, data collection, and analysis were performed by Takaharu Kudoh, Akihiro Haga, Keiko Kudoh, Akira Takahashi, Motoharu Sasaki, Yasusei Kudo, Hitoshi Ikushima, and Youji Miyamoto. The first draft of the manuscript was written

by Takaharu Kudoh, and all authors commented on the previous versions of the manuscript. All authors read and approved the final manuscript.

Acknowledgments

We thank Dr. Noriaki Takeda and Dr. Makoto Fukui for their scientific advice.

Radiomics analysis of [^{18}F]-fluoro-2-deoxyglucose positron emission tomography for the prediction of cervical lymph node metastasis in tongue squamous cell carcinoma

Abstract

Objectives

This study aimed to create a predictive model for cervical lymph node metastasis (CLNM) in patients with tongue squamous cell carcinoma (SCC) based on radiomics features detected by [^{18}F]-fluoro-2-deoxyglucose (^{18}F-FDG) positron emission tomography (PET).

Methods

A total of 40 patients with tongue SCC who underwent ^{18}F-FDG PET imaging during their first medical examination were enrolled. During the follow-up period (mean 28 months), 20 patients had CLNM, including six with late CLNM, whereas the remaining 20 patients did not have CLNM. Radiomics features were extracted from ^{18}F-FDG PET images of all patients irrespective of metal artifact, and clinicopathological factors were obtained from the medical records. Late CLNM was defined as the CLNM that occurred after major treatment. The least absolute shrinkage and selection operator (LASSO) model was used for radiomics feature selection and sequential data fitting. The receiver operating characteristic curve analysis was used to assess the predictive performance of the ^{18}F-FDG PET-based model and clinicopathological factors model (CFM) for CLNM.

Results

Six radiomics features were selected from LASSO analysis. The average values of the area under the curve (AUC), accuracy, sensitivity, and specificity of radiomics analysis for predicting CLNM from ^{18}F-FDG PET images were 0.79, 0.68, 0.65, and 0.70, respectively. In contrast, those of the CFM were 0.54, 0.60, 0.60, and 0.60, respectively. The ^{18}F-FDG PET-based model showed significantly higher AUC than that of the CFM.

Conclusions

The ^{18}F-FDG PET-based model has better potential for diagnosing CLNM and predicting late CLNM in patients with tongue SCC than the CFM.

Keywords

tongue squamous cell carcinoma; cervical lymph node metastasis; radiomics; [^{18}F]-fluoro-2-deoxyglucose, positron emission tomography

Introduction

Cervical lymph node metastasis (CLNM) is a major cause of mortality in patients with tongue squamous cell carcinoma (SCC). Diagnostic imaging has played an important role in the detection of CLNM in patients with tongue SCC. Routine radiological diagnosis of CLNM upon first medical examination has become more effective when used in combination with computed tomography (CT), ultrasonography (US), magnetic resonance imaging (MRI), or [^{18}F]-fluoro-2-deoxyglucose (^{18}F-FDG) positron emission tomography (PET) [1-4]. Regarding the management of CLNM, therapeutic neck dissection (ND) is adopted for clinically CLNM-positive neck patients, and elective ND for clinical T (cT)3-4N0M0 patients and sometimes for cT1-2N0 patients according to the National Comprehensive Cancer Network (NCCN) clinical practice guidelines [5]. Additionally, D'Cruz *et al*. [6] reported a survival benefit of elective ND compared with the wait-and-see policy in patients with early-stage oral SCC.

There is currently no method for evaluating the probability of CLNM or late CLNM occurrence. Patients with early-stage oral SCC on the wait-and-see policy have a CLNM rate of 20–40% [7-9]. In other words, approximately 60–80% of patients with early-stage oral SCC undergoing elective ND would experience unnecessary operative stress. Furthermore, clinically CLNM-positive patients who undergo therapeutic ND might be pathologically CLNM-negative (pN0) because routine radiological CLNM diagnosis for patients with oral SCC is not 100% accurate. As a result, pN0 patients could undergo an unnecessary ND operation, thus adding unwarranted operational stress. Therefore, a modality that facilitates both an accurate diagnosis

of CLNM and a prediction of late CLNM is required.

In recent years, the use of data characterization algorithms to extract information from radiological images for radiomics analysis has been highlighted. For example, Zhong *et al.* [10] and Cui *et al*. [11] predicted lymph node metastasis with high accuracy using images of primary lesions in patients with lung and breast cancer. Therefore, we hypothesized that radiomics analysis of medical images from the initial examination of primary lesions in patients with tongue SCC could predict CLNM.

The current radiologic modalities for patients with tongue SCC are CT, MRI, and ^{18}F-FDG PET/CT. ^{18}F-FDG PET/CT is often used in tongue cancer for locoregional diagnosis and for screening distant metastases or other malignancies because oral SCC can easily progress into multiple cancers in the oral cavity, pharynx, larynx, and esophagus [12, 13]. Moreover, ^{18}F-FDG PET images of primary lesions can be clearly delineated using the standardized uptake value (SUV) as a threshold. However, the images of oral sites are often affected by metal artifacts because dental metals are often used for oral restorations. Therefore, we hypothesized that radiomics analysis of the initial ^{18}F-FDG PET images of primary lesions in patients with tongue SCC would predict CLNM. Clinicopathological factors, depth of invasion (DOI) [5, 12, 13], and the Yamamoto–Kohama (YK) classification [14] were also assessed to predict CLNM occurrence in patients with tongue SCC, thereby verifying the prediction of CLNM for patients with tongue SCC using ^{18}F-FDG PET imaging of the primary lesions.

This study aimed to investigate initial medical examinations and follow-up data of patients with tongue

SCC on the wait-and-see policy, to establish appropriate treatment planning for patients with tongue SCC at the initial medical examination. Additionally, we verified the ability of radiomics analysis to predict CLNM in patients with tongue SCC by comparing the ^{18}F-FDG PET-based model with the clinicopathological factor model (CFM).

Materials and Methods

Ethics

This study was approved by the ethical committee of our hospital. The medical treatment protocol used by our hospital followed the Japanese Society of Oral Oncology guidelines or Japanese Society for Head and Neck Cancer Guidelines for the Treatment of Oral Cancer, and informed consent was obtained from all participants [12, 13].

Study participants

Patients with histologically diagnosed tongue SCC who underwent ^{18}F-FDG PET examination before major treatment between September 2015 and January 2019 at our hospital were reviewed. Major treatment referred to definitive therapy, surgery, or definitive radiotherapy [12, 13]. No patient received any previous treatment. Forty tongue SCC patients were enrolled for the study. The patient characteristics are shown in Table 1. There were 27 male patients and 13 female patients. The mean age of the patients was 66 years. Patients' distribution by cT classification and stage are shown in Table 1. Regarding the stage, patients who were staged according to the UICC TNM Classification of Malignant Tumours (7th edition), were restaged

using the 8th edition, for the purpose of this study. The mean DOI of the patients was 9 mm. The treatment modalities according to the neck status are summarized in Table 2. Of the 33 patients that underwent radical surgery for primary lesions, eight and six underwent therapeutic and elective ND, respectively. The remaining 19 patients who underwent radical surgery for primary lesions followed a wait-and-see policy and did not undergo ND. Of these 19, six patients had late CLNM while seven patients underwent definitive radiotherapy. Of the seven, six were CLNM-positive at the initial radiologic and/or clinical examination. Overall, CLNM occurred in 20 patients on the ipsilateral side. This study was designed based on a predictive AUC for CLNM of 0.75 (both 20 CLMN-positive and 20 CLMN-negative patients), using a receiver operating characteristic (ROC) curve, one-tailed, a sample power of 0.90, and at a significant level of 0.05. The median follow-up period was 28 months (range 1–61 months).

^{18}F-FDG PET/CT scan and data acquisition

^{18}F-FDG was synthesized by the nucleophilic substitution method using an ^{18}F-FDG-synthesizing instrument (F100, Sumitomo Heavy Industries, Ltd., Tokyo, Japan) at our hospital. All patients fasted for at least 6 h before undergoing ^{18}F-FDG PET/CT and were administered a dose of 3.0 MBq/kg of body weight 1 h before the scan. All imaging procedures were performed using an in-line PET/CT system on Aquiduo (PCA-7000B, Toshiba Medical Systems, Otawara, Tochigi, Japan). Images from eight-bed positions for two minutes each were obtained using a three-dimensional (3D) high-sensitivity mode.

Patients were scanned from the top of the skull to the upper thigh. The ^{18}F-FDG PET images were reconstructed into a 192 × 192 matrix using an ordered-subset expectation maximization iterative reconstruction algorithm called VUE Point FX (GE Healthcare, Milwaukee, WI, USA) with time-of-flight and sharp infrared spectroscopy (16 subsets, two iterations each). Noise in the resultant images was reduced through Gaussian smoothing at 4.0 mm full-width at half-maximum (F100, Sumitomo Heavy Industries, Ltd., Tokyo, Japan). Emission PET images were reconstructed using a default vender-implemented iterative reconstruction algorithm.

Extraction of radiomics features from ^{18}F-FDG PET images

Radiomics features of the primary lesions were analyzed using ^{18}F-FDG PET images obtained before major treatment. The ^{18}F-FDG PET images were extracted semi-automatically from picture archiving and communication systems. The region of interest (ROI) was set semi-automatically with an SUV of 2.5, indicating manual deletion of the normal physiological uptake, such as the tonsils by an oral radiation oncologist (TK), and an additive margin of 15 mm by automatically using Velocity™ (Varian Medical Systems, Palo Alto, CA) for compensation of the so-called clinical target volume (CTV) area (Fig. 1). Quantitative imaging features were evaluated using the ROI. Additionally, ^{18}F-FDG PET images were standardized as a preprocessing step for radiomics analysis. The voxel size of the ^{18}F-FDG PET images was 2 × 2 × 2 mm and resized to 3 × 3 × 3 mm. Thereafter, a 3D wavelet transform was applied to each image. The re-quantization with the 10- and 20-bin widths was performed in the 3D wavelet-transformed images,

as well as in the original image. Thus, four combinations of ROIs (2 mm-10-bin, 2 mm-20-bin, 3 mm-10-bin, and 3 mm-20-bin) were evaluated. We modified MATLAB programming tools (https://github.com/mvallieres/radiomics/) to extract 476 radiomics features from the ^{18}F-FDG PET images [15, 16]. Table 3 presents the radiomics features used in this study. Features based on eight shapes/sizes were calculated using MATLAB programming tools; 10 global, 11 GLCM (gray-level co-occurrence matrix), 13 GLRLM (gray-level run-length matrix), 13 GLSZM (gray-level size zone matrix), and 5 NGTDM were calculated using the SUV value, and 3D wavelet transformation was performed on the PET images using MATLAB programming tools. These radiomics features were labeled by the low-pass and/or high-pass functions used in the 3D wavelet transform. For example, ‘‘LHH_X’’ is the feature X with the image filtered with the low-pass function for the x **(**left-right) direction, the high-pass function for the y (antero-posterior) direction, and high-pass function for the z (head-tail) direction. Eight 3D wavelet features were generated from 52 features. The total features were eight shapes/sizes, 10 global, 11 GLCM, 13 GLRLM, 13 GLSZM, and 5 NGTDM (neighborhood gray-tone difference matrix). Finally, we modified MATLAB programming tools (https://github.com/mvallieres/radiomics/) to extract 476 radiomics features from the ^{18}F-FDG PET images (Table 3) and normalized the features using two statistical methods: min-max and z-score [15, 16].

Radiomics feature selection and multivariate analysis of ^{18}F-FDG PET-based model

Not all extracted radiomics features are always effective in predicting late CLNM in patients with tongue

SCC. Thus, we used the least absolute shrinkage and selection operator (LASSO) model to select only the effective radiomics features for use in the analysis. The LASSO model is an embedded method that simultaneously performs radiomics feature selection and data fitting, providing the radiomics features selected during the fitting, as well as the classification model fitted to the training data. Furthermore, five-fold cross-validation was employed to avoid overlearning, a common problem in model fitting. The prediction model was used in the training cohort (32 data points) and was evaluated in the test cohort (eight data points). The area under the ROC curve, accuracy, sensitivity, and specificity were analyzed. The hyperparameters were optimized with leave-one-out (LOO) validation in the training cohort. Furthermore, with the five-fold cross-validation using the LASSO method, radiomics feature selection was also performed five times with the different training cohorts. We used the glmnet and ROCR libraries of the R 2.7.0 software (https://cran-archive.r-project.org/bin/windows/base/old/2.7.0/) to evaluate the effective radiomics features for predicting late CLNM by counting the number of selections.

Multivariate analysis of CFM

Regarding clinicopathological factors, sex, age, cT classification, and radiological DOI (rDOI) were obtained from the medical records. rDOI was selected because pathological DOI (pDOI) could only be obtained after surgery. Tumor differentiation and YK classification were performed by an experienced oral pathologist (YK). Clinicopathological factors are listed in Table 4. There was no need to select the radiomics features in the CFM; therefore, the ridge model was applied. The ridge model differs from the LASSO

model in the penalty term only; the ridge model has an L2 norm, whereas the LASSO model has an L1 norm. The CFM was created using the same techniques as the ^{18}F-FDG PET-based model: five-fold cross-validation was performed, LOO validation was used for hyperparameter optimization, and R 2.7.0 software was utilized.

Multivariate analysis of radiomics features from ^{18}F-FDG PET images and the clinicopathological factors

We used six clinicopathological factors and 476 radiomics features of ^{18}F-FDG PET that were selected and analyzed using the aforementioned methods. The ROC curve and integrated discrimination index (IDI) were calculated to compare the predictive performance of the radiomics features and CFM of CLNM in patients with tongue SCC.

Results

Radiomics feature selection and multivariate analysis of ^{18}F-FDG PET-based model

Regarding histogram-based radiomics features from ^{18}F-FDG PET images, LHLMax as a global type feature was selected five times in the five-fold cross-validation from LASSO analysis. LHLMax is the feature of the highest SUV filtered with the low-pass function for the x (left-right) direction, high-pass function for the y (antero-posterior) direction, and low-pass function for the z (head-tail) direction. The following global type features were selected two times: (1) HHHMean and LHHMean and (2) HHHZLV, HHHRLV, and HHHLRHGE as GLRLM type features. The mean is the feature of the mean SUV, and

GLRLM comprises counting the number of pixel segments having the same intensity in a given direction. Thus, we determined LHLMax to be the radiomics feature with the strongest correlation with late CLNM. Based on five-fold cross-validation, data from 32 participants were used as training data, whereas data from 8 participants were used as testing data. The average area under the curve (AUC) in the ROC curve, accuracy, sensitivity and specificity with one standard deviation of radiomics analysis are shown in Table 5. The AUC, accuracy, sensitivity, and specificity ranged from 0.65 to 0.79, 0.53 to 0.68, 0.50 to 0.70, and 0.55 to 0.70, respectively.

Multivariate analysis of CFM

The neck status according to each clinicopathological factor is summarized in Table 6. The average AUC, accuracy, sensitivity, and specificity curves of all six clinicopathological factors were lower than those of the radiomics features from ^{18}F-FDG PET images (Table 7).

Multivariate analysis of radiomics features from ^{18}F-FDG PET images and the clinicopathological factors

The six clinicopathological factors were not selected in the LASSO analysis, whereas the radiomics features were. The AUC, accuracy, sensitivity, and specificity of multivariate analysis of both the radiomics and clinicopathological factors were the same as those of only the radiomics features. The ROC curves of both radiomics features and all six clinicopathological factors were plotted to validate their predictive ability of

neck status (Fig. 2). Radiomics analysis of ^{18}F-FDG PET images had a significantly higher AUC than the CFM (IDI 0.02).

Discussion

In this study, we aimed to verify the ability of radiomics analysis of ^{18}F-FDG PET images of primary lesions to predict the occurrence of CLNM in patients with tongue SCC by comparison with a CFM. The first stage of our investigation was the evaluation of the radiomics analysis of ^{18}F-FDG PET. The very high sensitivity of primary lesions to ^{18}F-FDG PET has been reported in head and neck cancers, including tongue SCC [17, 18]. In particular, SUV is reported to be the primary quantitative indicator for tumor detection using ^{18}F-FDG-PET [19, 20], and the smallest SUVmax of the primary lesions in all 40 patients was 3.2 in this study. Lee *et al.* reported that patients with an SUV threshold of 2.5 or higher showed a worse prognosis [21]. Therefore, a threshold value of 2.5 was considered to be appropriate to depict the primary lesion. Regarding the margin setting, the Radiation Therapy Oncology Group protocols expand the gross tumor volume (GTV) area by 10–20 mm to predict the CTV area [22]. Merlotti *et al*. reported that a 15 mm margin around the GTV was preferable [23]. Therefore, we evaluated the region that provided a margin of 15 mm to the ^{18}F-FDG uptake area.

Moreover, we observed and selected six radiomics features for LASSO analysis. Of these, LHLMax was the most significant radiomics feature for predicting CLNM in patients with tongue SCC as the global type of feature. LHLMax and the other Max features, except HHHMax, showed a correlation coefficient greater

than 0.7 and similar tendencies. This may suggest that primary lesions with a higher SUV in ^{18}F-FDG PET images are more likely to indicate CLNM in patients with tongue SCC because Max expresses the highest SUV. Additionally, H of LHL is the y-direction, which indicates the antero-posterior dimension. In this study, the maximal diameter at the y-dimension was observed in 34 of 40 patients, although the reason remains unclear.

Regarding the application of radiomics analysis of ^{18}F-FDG PET images in head and neck cancer [24-27], this study is the first to report the use of ^{18}F-FDG PET imaging of the primary lesions to predict CLNM. Although the application of radiomics analysis of CT images of head and neck cancer has been reported previously [28-30], these reports focus mostly on the prognosis and distant metastasis of head and neck cancer, not CLNM. Romeo *et al*. [30] achieved a predictive accuracy for CLNM of 90% by radiomics analysis of CT images of primary lesions of 40 patients with oropharyngeal and oral SCC. However, the primary lesions in the CT images could not be delineated in our 19 / 40 (47.5%) patients owing to the presence of metal artifacts, and Romeo *et al*. also excluded 10 (25.0%) patients with motion or beam-hardening artifacts and those with no detection of tumor lesions. Therefore, the practicality of the application of radiomics analysis of CT images of head and neck cancer has a problem. To improve the quality of CT images when metal artifacts are present, image processing, such as single-energy metal artifact reduction (SEMAR), has been recently used [31]. SEMAR has been used in our hospital for diagnostic CT scans. However, quantitative analysis of SEMAR images is difficult because the metal

artifact is imperfectly removed, and the comparison between SEMAR and non-SEMAR images is not yet been compared. Metal artifacts are also an obstacle in diagnosis using MRI [32, 33].

We used clinicopathological factors, including rDOI, cT classification, tumor differentiation, YK classification, gender, and age, as controls. pDOI was the best predictor of late CLNM according to the NCCN clinical practice guidelines [5]. ND is only recommended in highly selective situations where the pDOI is less than 2 mm; clinical judgment (regarding the reliability of follow-up, clinical suspicion, and other factors) must be exercised to determine the appropriateness of ND for a pDOI of 2–4 mm [5]. Huang *et al*. reported a DOI cut-off of 4 mm as the best predictive value for CLNM in patients with tongue SCC, with a pooled negative predictive value of > 95% [34]. However, Bur *et al*. [35] developed and validated machine learning algorithms to predict pathological CLNM using pDOI in 1961 patients with T1-2N0 oral SCC from the National Cancer Database and 71 patients with T1-2N0 oral SCC from their institution. They reported that these machine learning algorithms had a predictive AUC of 0.657 for pathologic CLNM in patients with cT1-2N0 oral SCC, similar to our results. In addition, the correlation between CLNM and T stage remains controversial [36-41]. Nevertheless, the T stage is considered the most reliable predictor of survival and locoregional control in NCCN clinical practice guidelines [5]. Regarding tumor differentiation, patients with poorly differentiated tumors had a higher incidence of CLNM than those with well-differentiated tumors [39, 42, 43]. In this study, only one of the 40 patients with tongue SCC presented with a poorly differentiated tumor. Additionally, Kurokawa *et al*. [44] reported that moderately differentiated

tongue SCC with a tumor depth of at least 4 mm had predictive value for late CLNM. However, Shin *et al.* reported no correlation between tumor differentiation and the incidence of late CLNM (P = 0.698) [41]. The YK classification used in this study is a modified version of that used by Jakobsson *et al*. [45] and Willen *et al.* [46]; these studies focused on the pattern of invasion at tumor margins. The YK classification was reported as a predictor of CLNM [47, 48] and has been widely used in Japan for oral cancers since 1984, when Yamamoto *et al*. [14] reported that grades 4C and 4D had a high frequency of metastasis (4C: 11/18,61.1%; 4D: 9/12,75.0%; total: 20/30,66.7%). They also revealed that the presence of metastasis indicates a poorer prognosis than did the absence of the mode of invasion in each grade, especially in grades 4C and 4D. However, in 2014, Shinozaki *et al.* reported no significant differences between YK grades with respect to CLNM occurrence [49]. Other clinicopathological factors of CLNM, such as CD105 and vascular endothelial growth factor [50], low expression of E-cadherin [51], matrix metalloproteinase-2 [52], CD31 and PROX1 [53], lymphocytic host response, and tumor budding [54], have been previously reported in patients with oral SCC. Mermod *et al.* [53] assessed the overall performance of CD31, PROX1, and relevant histological parameters in 168 patients with early-stage oral SCC (AUC = 0.89, accuracy = 0.88). Meanwhile, Shan *et al.* reported the predictive performance of pDOI, pattern of invasion, lymphocytic host response, and tumor budding (AUC = 0.96) for CLNM before surgery in 145 patients with early-stage tongue SCC [54]. The predictive performance of the six clinicopathological factors used in this study was less satisfactory than that in the previous report. Further studies, including variables, such as tumor budding,

are warranted to improve the predictive performance of multivariate analysis of radiomics features from ^{18}F-FDG PET images and the clinicopathological factors. However, our results indicate that the AUC, accuracy, sensitivity, and specificity of CFMs were significantly lower than those of the ^{18}F-FDG PET-based model.

To our knowledge, this is the first study to evaluate the predictive performance for CLNM of radiomics analysis of primary lesions from ^{18}F-FDG PET images in patients with tongue SCC. Our findings demonstrated that the probability of the CLNM, including that of late CLNM, in patients with tongue SCC could be quantified using radiomics analysis of the initial ^{18}F-FDG PET examination. Additionally, we showed that radiomics analysis could predict the occurrence of CLNM in patients with tongue SCC.

This study had some limitations. The difference in the predictive performance between CLNM-positive at the initial medical examination and late CLNM occurrence in patients could not be examined because the sample size was small. To increase the sample size, studies conducted in multi-institutional cohorts should be performed using our radiomics analysis model. Furthermore, standardization of both ^{18}F-FDG PET/CT scanning and data acquisition is warranted to improve the predictive ability of radiomics analysis [55].

In conclusion, this study demonstrated that radiomics analysis of primary lesions using 18F-FDG PET imaging, which is not affected by metal artifacts, has better potential for diagnosing CLNM and predicting late CLNM in patients with tongue SCC than the CFM.

References

1. Castelijns JA, van den Brekel MW. Detection of lymph node metastases in the neck: radiologic criteria. AJNR Am J Neuroradiol. 2001;22:3–4. https://doi.org/10.1148/radiology.192.3.8058923

2. Eida S, Sumi M, Yonetsu K, Kimura Y, Nakamura T. Combination of helical CT and Doppler sonography in the follow-up of patients with clinical N0 stage neck disease and oral cancer. AJNR Am J Neuroradiol. 2003;24:312–8

3. Schöder H, Carlson DL, Kraus DH, Stambuk HE, Gönen M, Erdi YE, et al. 18F-FDG PET/CT for detecting nodal metastases in patients with oral cancer staged N0 by clinical examination and CT/MRI. J Nucl Med. 2006;47:755–62

4. Pandeshwar P, Jayanthi K, Raghuram P. Pre-operative contrast enhanced computer tomographic evaluation of cervical nodal metastatic disease in oral squamous cell carcinoma. Indian J Cancer. 2013;50:310–5. https://doi.org/10.4103/0019-509X.123605

5. Pfister DG, Ang K, Brizel DM, Burtness BA, Cmelak AJ, Colevas AD, et al. Head and Neck Cancers, version 3.2021, NCCN clinical practice guidelines in oncology. Accessed 20 Sep 2021. http://www.nccn.org/guidelines/guidelines-detail?category=1&id=1437;9:596–650;9:596–650. https://doi.org/10.6004/jnccn.2011.0053

6. D'Cruz AK, Vaish R, Kapre N, Dandekar M, Gupta S, Hawaldar R, et al. Elective versus therapeutic

neck dissection in node-negative oral cancer. N Engl J Med. 2015;373:521–9. https://doi.org/10.1056/NEJMoa1506007

7. Yuen AP, Wei WI, Wong YM, Tang KC. Elective neck dissection versus observation in the treatment of early oral tongue carcinoma. Head Neck. 1997;19:583–8. https://doi.org/10.1002/(SICI)1097-0347(199710)19:7<583::AID-HED4>3.0.CO;2-3

8. Lim YC, Lee JS, Koo BS, Kim SH, Kim YH, Choi EC. Treatment of contralateral N0 neck in early squamous cell carcinoma of the oral tongue: elective neck dissection versus observation. Laryngoscope. 2006;116:461–5. https://doi.org/10.1097/01.mlg.0000195366.91395.9b

9. Kelner N, Vartanian JG, Pinto CA, Coutinho-Camillo CM, Kowalski LP. Does elective neck dissection in T1/T2 carcinoma of the oral tongue and floor of the mouth influence recurrence and survival rates? Br J Oral Maxillofac Surg. 2014;52:590–7. https://doi.org/10.1016/j.bjoms.2014.03.020

10. Zhong Y, Yuan M, Zhang T, Zhang YD, Li H, Yu TF. Radiomics approach to prediction of occult mediastinal lymph node metastasis of lung adenocarcinoma. AJR Am J Roentgenol. 2018;211:109–13. https://doi.org/10.2214/AJR.17.19074

11. Cui X, Wang N, Zhao Y, Chen S, Li S, Xu M, et al. Preoperative prediction of axillary lymph node metastasis in breast cancer using radiomics features of DCE-MRI [Sci. rep.:2240]. Sci Rep. 2019;9:2240. https://doi.org/10.1038/s41598-019-38502-0

12. Japanese Society for Head and Neck cancer guidelines for the treatment of oral cancer. Accessed 30

Jun 2021. http://www.jsco-cpg.jp/headandneck-cancer/algo/#III-B-1

13. Japanese Society of Oral Oncology guidelines for the treatment of oral cancer. Accessed 30 Jun 2021. https://www.jstage.jst.go.jp/article/jsot1989/19/3/19_3_139/_pdf/-char/ja

14. Yamamoto E, Miyakawa A, Kohama G. Mode of invasion and lymph node metastasis in squamous cell carcinoma of the oral cavity. Head Neck Surg. 1984;6:938–47. https://doi.org/10.1002/hed.2890060508

15. Vallières M, Freeman CR, Skamene SR, El Naqa I. A radiomics model from joint FDG-PET and MRI texture features for the prediction of lung metastases in soft-tissue sarcomas of the extremities. Phys Med Biol. 2015;60:5471–96. https://doi.org/10.1088/0031-9155/60/14/5471

16. Haga A, Takahashi W, Aoki S, Nawa K, Yamashita H, Abe O, et al. Classification of early stage non-small cell lung cancers on computed tomographic images into histological types using radiomic features: interobserver delineation variability analysis. Radiol Phys Technol. 2018;11:27–35. https://doi.org/10.1007/s12194-017-0433-2

17. Di Martino E, Nowak B, Hassan HA, Hausmann R, Adam G, Buell U, et al. Diagnosis and staging of head and neck cancer: a comparison of modern imaging modalities (positron emission tomography, computed tomography, color-coded duplex sonography) with panendoscopic and histopathologic findings. Arch Otolaryngol Head Neck Surg. 2000;126:1457–61. https://doi.org/10.1001/archotol.126.12.1457

18. Ahn PH, Garg MK. Positron emission tomography/computed tomography for target delineation in head and neck cancers. Semin Nucl Med. 2008;38:141–8. https://doi.org/10.1053/j.semnuclmed.2007.11.002

19. Houweling AC, Wolf AL, Vogel WV, Hamming-Vrieze O, van Vliet-Vroegindeweij CV, van de Kamer JB, et al. FDG-PET and diffusion-weighted MRI in head-and-neck cancer patients: implications for dose painting. Radiother Oncol. 2013;106:250–54. https://doi.org/10.1016/j.radonc.2013.01.003

20. Yan O, Wang H, Han Y, Fu S, Chen Y, Liu F. Prognostic relevance of 18F-FDG-PET/CT-guided target volume delineation in loco-regionally advanced nasopharyngeal carcinomas: a comparative study. Front Oncol. 2021;11:709622. https://doi.org/10.3389/fonc.2021.709622

21. Lee SJ, Choi JY, Lee HJ, Baek CH, Son YI, Hyun SH, et al. Prognostic value of volume-based ^{18}F-fluorodeoxyglucose PET/CT parameters in patients with clinically node-negative oral tongue squamous cell carcinoma. Korean J Radiol. 2012;13:752–9. https://doi.org/10.3348/kjr.2012.13.6.752

22. Thomas TO, Refaat T, Choi M, Bacchus I, Sachdev S, Rademaker AW, et al. Brachial plexus dose tolerance in head and neck cancer patients treated with sequential intensity modulated radiation therapy. Radiat Oncol. 2015;10:94. https://doi.org/10.1186/s13014-015-0409-5

23. Merlotti A, Alterio D, Vigna-Taglianti RV, Muraglia A, Lastrucci L, Manzo R, et al. Technical guidelines for head and neck cancer IMRT on behalf of the Italian association of radiation oncology - head and neck working group. Radiat Oncol. 2014;9:264. https://doi.org/10.1186/s13014-014-0264-9

24. Zhou Z, Chen L, Sher D, Zhang Q, Shah J, Pham NL, et al. Predicting lymph node metastasis in head and neck cancer by combining many-objective radiomics and 3-dimensioal convolutional neural network through evidential reasoning. Annu Int Conf IEEE Eng Med Biol Soc. Annu international conference IEEE Eng Med Biol Soc Annu international conference IEEE Eng Med Biol Soc. 2018;2018:1–4. https://doi.org/10.1109/EMBC.2018.8513070

25. Haider SP, Zeevi T, Baumeister P, Reichel C, Sharaf K, Forghani R, et al. Potential Added Value of PET/CT Radiomics for Survival Prognostication beyond AJCC 8th Edition Staging in Oropharyngeal Squamous Cell Carcinoma. Cancers (Basel). 8th ed. 8th ed. 2020;12:1778. https://doi.org/10.3390/cancers12071778

26. Martens RM, Koopman T, Noij DP, Pfaehler E, Übelhör C, Sharma S, et al. Predictive value of quantitative ^{18}F-FDG-PET radiomics analysis in patients with head and neck squamous cell carcinoma. EJNMMI Res. 2020;10:102. https://doi.org/10.1186/s13550-020-00686-2

27. Chen L, Zhou Z, Sher D, Zhang Q, Shah J, Pham NL, et al. Combining many-objective radiomics and 3D convolutional neural network through evidential reasoning to predict lymph node metastasis in head and neck cancer. Phys Med Biol. 2019;64:075011. https://doi.org/10.1088/1361-6560/ab083a

28. Zhai TT, Langendijk JA, van Dijk LV, Halmos GB, Witjes MJH, Oosting SF, et al. The prognostic value of CT-based image-biomarkers for head and neck cancer patients treated with definitive (chemo-)radiation. Oral Oncol. 2019;95:178–86. https://doi.org/10.1016/j.oraloncology.2019.06.020

29. Diamant A, Chatterjee A, Vallières M, Shenouda G, Seuntjens J. Deep learning in head & neck cancer outcome prediction [Sci. rep.:2764]. Sci Rep. 2019;9:2764. https://doi.org/10.1038/s41598-019-39206-1

30. Romeo V, Cuocolo R, Ricciardi C, Ugga L, Cocozza S, Verde F, et al. Prediction of tumor grade and nodal status in oropharyngeal and oral cavity squamous-cell carcinoma using a radiomic approach. Anticancer Res. 2020;40:271–80. https://doi.org/10.21873/anticanres.13949

31. Miki K, Mori S, Hasegawa A, Naganawa K, Koto M. Single-energy metal artefact reduction with CT for carbon-ion radiation therapy treatment planning. Br J Radiol. 2016;89:20150988. https://doi.org/10.1259/bjr.20150988

32. Arena L, Morehouse HT, Safir J. MR imaging artifacts that simulate disease: how to recognize and eliminate them. RadioGraphics. 1995;15:1373–94. https://doi.org/10.1148/radiographics.15.6.8577963

33. Kaneda T, Minami M, Curtin HD, Utsunomiya T, Shirouzu I, Yamashiro M, et al. Dental bur fragments causing metal artifacts on MR images. AJNR Am J Neuroradiol. 1998;19:317–9

34. Huang SH, Hwang D, Lockwood G, Goldstein DP, O'Sullivan B. Predictive value of tumor thickness for cervical lymph-node involvement in squamous cell carcinoma of the oral cavity: a meta-analysis of reported studies. Cancer. 2009;115:1489–97. https://doi.org/10.1002/cncr.24161

35. Bur AM, Holcomb A, Goodwin S, Woodroof J, Karadaghy O, Shnayder Y, et al. Machine learning to predict occult nodal metastasis in early oral squamous cell carcinoma. Oral Oncol. 2019;92:20–5. https://doi.org/10.1016/j.oraloncology.2019.03.011

36. Shaha AR, Spiro RH, Shah JP, Strong EW. Squamous carcinoma of the floor of the mouth. Am J Surg. 1984;148:455–9. https://doi.org/10.1016/0002-9610(84)90369-6

37. Spiro RH, Huvos AG, Wong GY, Spiro JD, Gnecco CA, Strong EW. Predictive value of tumor thickness in squamous carcinoma confined to the tongue and floor of the mouth. Am J Surg. 1986;152:345–50. https://doi.org/10.1016/0002-9610(86)90302-8

38. Rodolico V, Barresi E, Di Lorenzo R, Leonardi V, Napoli P, Rappa F, et al. Lymph node metastasis in lower lip squamous cell carcinoma in relation to tumour size, histologic variables and p27Kip1 protein expression. Oral Oncol. 2004;40:92–8. https://doi.org/10.1016/S1368-8375(03)00141-6

39. Umeda M, Yokoo S, Take Y, Omori A, Nakanishi K, Shimada K. Lymph node metastasis in squamous cell carcinoma of the oral cavity: correlation between histologic features and the prevalence of metastasis. Head Neck. 1992;14:263–72. https://doi.org/10.1002/hed.2880140402

40. Franceschi D, Gupta R, Spiro RH, Shah JP. Improved survival in the treatment of squamous carcinoma of the oral tongue. Am J Surg. 1993;166:360–5. https://doi.org/10.1016/S0002-9610(05)80333-2

41. Shin JH, Yoon HJ, Kim SM, Lee JH, Myoung H. Analyzing the factors that influence occult metastasis in oral tongue cancer. J Korean Assoc Oral Maxillofac Surg. 2020;46:99–107. https://doi.org/10.5125/jkaoms.2020.46.2.99

42. Frierson HF Jr, Cooper PH. Prognostic factors in squamous cell carcinoma of the lower lip. Hum Pathol. 1986;17:346–54. https://doi.org/10.1016/S0046-8177(86)80457-9

43. Sparano A, Weinstein G, Chalian A, Yodul M, Weber R. Multivariate predictors of occult neck metastasis in early oral tongue cancer. Otolaryngol Head Neck Surg. 2004;131:472–6. https://doi.org/10.1016/j.otohns.2004.04.008

44. Kurokawa H, Yamashita Y, Takeda S, Zhang M, Fukuyama H, Takahashi T. Risk factors for late cervical lymph node metastases in patients with stage I or II carcinoma of the tongue. Head Neck. 2002;24:731–6. https://doi.org/10.1002/hed.10130

45. Jakobsson PA, Eneroth CM, Killander D, Moberger G, Mårtensson B. Histologic classification and grading of malignancy in carcinoma of the larynx. Acta Radiol Ther Phys Biol. 1973;12:1–8. https://doi.org/10.3109/02841867309131085

46. Willén R, Nathanson A. Squamous cell carcinoma of the gingiva. Histological classification and grading of malignancy. Acta Oto-laryngol. 1973;75:299–300. https://doi.org/10.3109/00016487309139722

47. Yamane M, Ishii J, Izumo T, Nagasawa T, Amagasa T. Noninvasive quantitative assessment of oral

tongue cancer by intraoral ultrasonography. Head Neck. 2007;29:307–14. https://doi.org/10.1002/hed.20523

48. Kaneoya A, Hasegawa S, Tanaka Y, Omura K. Quantitative analysis of invasive front in tongue cancer using ultrasonography. J Oral Maxillofac Surg. 2009;67:40–6. https://doi.org/10.1016/j.joms.2007.08.006

49. Shinozaki Y, Jinbu Y, Ito H, Noguchi T, Kusama M, Matsumoto N, et al. Relationship between appearance of tongue carcinoma on intraoral ultrasonography and histopathologic findings. Oral Surg Oral Med Oral Pathol Oral Radiol. 2014;117:634–9. https://doi.org/10.1016/j.oooo.2014.02.001

50. Chien CY, Su CY, Hwang CF, Chuang HC, Chen CM, Huang CC. High expressions of CD105 and VEGF in early oral cancer predict potential cervical metastasis. J Surg Oncol. 2006;94:413–7. https://doi.org/10.1002/jso.20546

51. Lim SC, Zhang S, Ishii G, Endoh Y, Kodama K, Miyamoto S, et al. Predictive markers for late cervical metastasis in stage I and II invasive squamous cell carcinoma of the oral tongue. Clin Cancer Res. 2004;10:166–72. https://doi.org/10.1158/1078-0432.CCR-0533-3

52. Gontarz M, Wyszyńska-Pawelec G, Zapała J, Czopek J, Lazar A, Tomaszewska R. Immunohistochemical predictors in squamous cell carcinoma of the tongue and floor of the mouth. Head Neck. 2016;38;Suppl 1:E747–53. https://doi.org/10.1002/hed.24087

53. Mermod M, Jourdan EF, Gupta R, Bongiovanni M, Tolstonog G, Simon C, et al. Development and

validation of a multivariable prediction model for the identification of occult lymph node metastasis in oral squamous cell carcinoma. Head Neck. 2020;42:1811–20. https://doi.org/10.1002/hed.26105

54. Shan J, Jiang R, Chen X, Zhong Y, Zhang W, Xie L, et al. Machine learning predicts lymph node metastasis in early-stage oral tongue squamous cell carcinoma. J Oral Maxillofac Surg. 2020;78:2208–18. https://doi.org/10.1016/j.joms.2020.06.015

55. Yip SS, Aerts HJ. Applications and limitations of radiomics. Phys Med Biol. 2016;61:R150–66. https://doi.org/10.1088/0031-9155/61/13/R150

Figure captions

Fig. 1 Primary lesion analyzed using 18F-FDG PET images. (a) The 18F-FDG PET CT image, (b) the region with SUV ≥2.5 (red area), and the region with a margin of 15 mm (blue area). CT, computed tomography; 18F-FDG, [^{18}F]-fluoro-2-deoxyglucose; PET, positron emission tomography; SUV, standardized uptake value.

Fig. 2 ROC curves of radiomics features using ^{18}F-FDG PET and clinicopathological factors. Radiomics feature analysis is represented by the red line, whereas the clinicopathological factors are represented by the black line. ROC, receiver operating characteristic; ^{18}F-FDG, [^{18}F]-fluoro-2-deoxyglucose; PET, positron emission tomography

Table 1. Patient characteristics.

Characteristics	Total
Sex	
Male	27
Female	13
Age (years)*	66±14
Clinical T classification	
1	7
2	12
3	13
4a	7
4b	1
Stage	
Ⅰ	6
Ⅱ	12
Ⅲ	7
Ⅳa	13
Ⅳb	2
DOI, mm	9±6

*mean ± standard deviation

DOI, depth of invasion

Table 2. The neck status of patients according to treatment modalities

Treatment modality	Neck status	
	Positive	Negative
Treatment modality		
Therapeutic neck dissection	8	0
Prophylactic neck dissection	0	6
Wait and see policy	6	13
Radiation	6	1

Table 3. Radiomics features analyzed in this study

Feature type	Feature name
Shape/size	Compactness1, Compactness2, MaxDiameter, SphericalDisproportion, Sphericity, SurfaceArea, SurfaceVolumeratio, Volume
Global	Variance, Skewness, Kurtosis, Energy, Max, Mean, median, Min, Uniformity, Entropy
GLCM	Energy, Contrast, Correlation1, Correlation2, Homegeneity1, Homogeneity2, variance, SumAverage, Entropy, Dissimilarity, AutoCorrelation
GLRLM	Short Run Emphasis (SRE), Long Run Emphasis (LRE), Gray-Level Non-uniformity (GLN), Run-Length Non-uniformity (RLN), Run Percentage (RP), Low Gray-Level Run Emphasis (LGRE), High Gray-Level Run Emphasis (HGRE), Short Run Low Gray-Level Emphasis (SRLGE), Short Run High Gray-Level Emphasis (SRHGE), Long Run Low Gray-Level Emphasis (LRLGE), Long Run High Gray-Level Emphasis (LRHGE), Gray-Level Variance (GLV), Run-Length Variance (RLV)
GLSZM	Small Zone Emphasis (SZE), Large Zone Emphasis (LZE), Gray-Level Non-uniformity (GLN), Zone-Size Non-uniformity (ZSN), Zone Percentage (ZP), Low Gray-Level Zone Emphasis (LGZE), High Gray-Level Zone Emphasis (HGZE), Small Zone Low Gray-Level Emphasis (SZLGE), Small Zone High Gray-Level Emphasis (SZHGE), Large Zone Low Gray-Level Emphasis (LZLGE), Large Zone High Gray-Level Emphasis (LZHGE), Gray-Level Variance (GLV), Zone-Size Variance (ZSV)
NGTDM	Coarseness, Contrast, Busyness, Complexity, Strength

GLCM gray-level co-occurrence matrix; GLRLM gray-level run-length matrix; GLSZM gray-level size zone matrix; NGTDM neighborhood gray-tone difference matrix

Table 4. Clinicopathological factors

Factors	Total
Differentiation	
Highly	20
Moderate	19
Poorly	1
Y-K classification	
2	2
3	14
4c	17
4d	7

Table 6. Clinicopathological characteristics of patients stratified by neck status.

	Neck status	
Characteristics	Positive	Negative
Sex		
Male	13	14
Female	6	7
Age (years)*	68±13	64±16
Clinical T classification		
1	2	5
2	5	7
3	7	6
4a	5	2
4b	1	0
Differentiation		
Highly	11	9
Moderate	8	11
Poorly	1	0
Y-K classification		
2	1	1
3	5	9
4c	12	5
4d	2	5
DOI, mm	10±7	8±5

*mean ± standard deviation;

DOI, depth of invasion

Table 5. AUC, accuracy, sensitivity, and specificity of the radiomics analysis in predicting CLMN

Dataset	AUC	Accuracy	Sensitivity	Specificity
2-mm 10-bin *Z*-score	0.75±0.13	0.68±0.13	0.70±0.10	0.65±0.20
3-mm 10-bin *Z*-score	0.79±0.10	0.68±0.13	0.65±0.12	0.70±0.19
2-mm 20-bin *Z*-score	0.65±0.27	0.53±0.24	0.50±0.27	0.55±0.25
3-mm 10-bin *Z*-score	0.75±0.14	0.65±0.12	0.60±0.12	0.70±0.19

AUC, area under the curve; CLMN; cervical lymph node metastasis.

Table 7

Table 7. AUC, accuracy, sensitivity, and specificity of the clinicopathological factors model in predicting metastasis.

AUC	Accuracy	Sensitivity	Specificity
0.54±0.08	0.60±0.05	0.60±0.20	0.60±0.12

AUC, area under the curve.

Figure 1

Fig 1

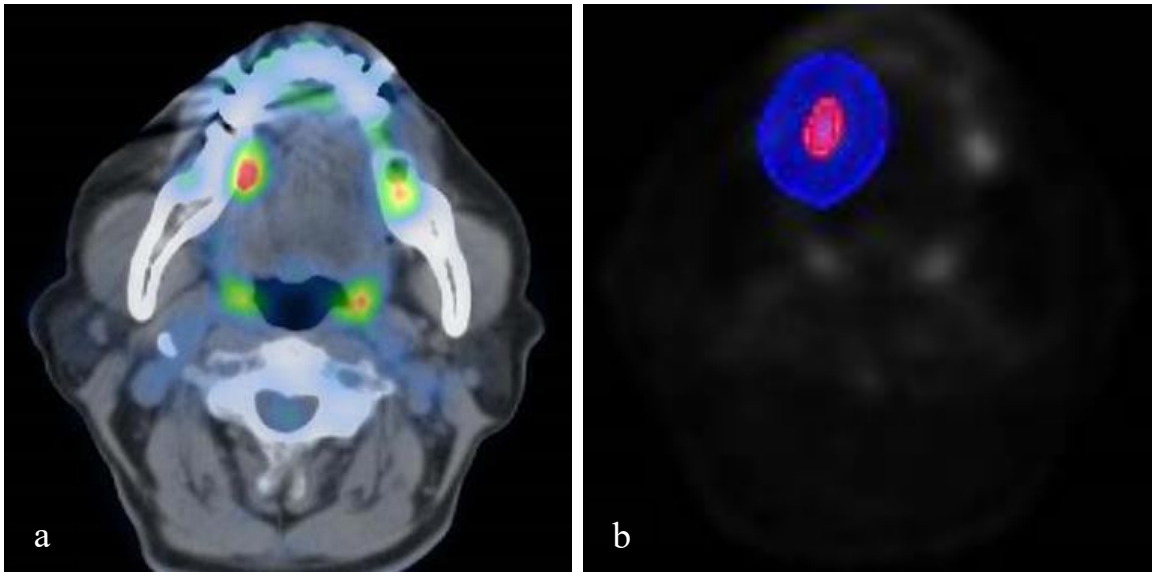

Figure 2

Fig 2